The Kihara Potential Function Parameters of Methane, Ethane, Propane, and i-Butane: The Effects on Clathrate Hydrate Structure Determination

Saeed Avaji [1], Jafar Javanmardi [1*] , Amir H. Mohammadi [2,*], Nejat Rahmanian [3], Vladislav De-Gald [3]

[1] Department of Chemical, Petroleum and Gas Engineering, Shiraz University of Technology, Shiraz, Iran

[2] Discipline of Chemical Engineering, School of Engineering, University of KwaZulu-Natal, Howard College Campus, King George V Avenue, Durban 4041, South Africa

[3] Department of Chemical Engineering, Faculty of Engineering and Informatics, University of Bradford, Bradford BD71DP, United Kingdom

***: Corresponding authors email addresses:** javanmardi@sutech.ac.ir and amir_h_mohammadi@yahoo.com

ABSTRACT

Gas hydrates, or clathrate hydrates, are solid crystalline compounds, which are mixtures of water and gas. Prediction of hydrate dissociation conditions of natural gases is important in separation processes, gas storage industries, and in preventing blockage of gas transmission pipelines. In this study, initially, the different sets of the Kihara Potential Function Parameters, KPFP, reported in the literature were used to predict the equilibrium dissociation conditions of available experimental data for methane, ethane, propane and i-butane hydrates and mixtures of these four compounds. In most cases, however, based on these sets of KPFP, the hydrate structure cannot be predicted correctly. Consequently due to incorrect estimation of the hydrate structure, especially for natural gas mixture, the predicted equilibrium conditions are incorrect. For overcoming this fault and using a genetic algorithm, a new set of KPFP were optimized based on the new definition of the objective function and considering of structurea . The results show good compatibility with experimental data, both in the prediction of hydrate dissociation conditions and hydrate structures.

Keywords: Gas hydrate; Clathrate hydrate; Kihara Potential Function Parameters; Genetic algorithm; Model; Optimization.

1. INTRODUCTION

Natural gas hydrate, or Clathrate hydrate, is a solid crystalline compound that consists of water and gas. Water molecules trap the guest molecules (gas) in the cavities generated by the hydrogen bonds between the host water molecules. Guest molecules are kept in the cavities due to the van der Waals forces, meaning that there are no chemical bonds. Guest molecules are usually small hydrocarbons such as methane, ethane, etc. Gas hydrates may cause some plugging problems in pipelines, vessels, valves and in general devices, especially at high pressure and low temperatures. This plugging may cause irreversible damages, such as an explosion in oil and gas industries. There is a thought that the cause of the Deepwater Horizon oil spill in the Gulf of Mexico in 2010 was the formation of hydrate.

For the first time, Muller and Stackleberg[1] studied the properties of the hydrate structures using X-ray. According to Muller and Stackelberg's experiments, two types of hydrate crystalline structures were identified known as structure I, sI, and structure II, sII hydrates. In 1987, Ripmeester et al.[2] found out that the structure H of gas hydrates were able to encage larger molecules. Light hydrocarbons and natural gas mixtures, usually, form Structure I or II.

The first step in the estimation of hydrate formation temperatures, especially for natural gas hydrates, is to determine which structure is formed. In the absence of the experimental data on the structure, commonly, the hydrate formation conditions for two structures are determined and the stable gas hydrate structure is the one in which its formation temperature (and/or pressure) is higher (and/or lower). Based on these criteria, some case , however, the predicted *hydrate structure* is not in accordance with experimental data and consequently, the predicted formation conditions are not in agreement with experimental values. Therefore, it is required to find a way which is able to predict the gas hydrate structure correctly.

Different thermodynamic models were proposed to predict the hydrate equilibrium conditions. At first, van der Waals and Platteeuw[3] (vdW-P) presented a statistical model for estimation of water chemical potential in the hydrate phase and using the Lenard-Jones potential function to calculate the Langmuir constant. McCoy and Sinanoğlu[4] suggested usingthe KPFP for larger and non-spherical molecules instead of the Lenard-Jones potential function. Parrish and Prausnitz[5] extended the vdW-P solid solution theory for gas mixtures and also the component fugacity was used instead of partial pressure of the components. They also proposed a relation for estimation of water chemical potential in the liquid phase to predict the hydrate equilibrium conditions. They also estimated KPFP for 15 different gases. Holder and Hand[6] in 1982, reported hydrate dissociation pressure for methane, ethane, propane, and their mixtures. They also optimized KPFP using experimental dissociation pressure. They reported that mixtures of these gases can form either sI or sII hydrates under different thermodynamic conditions. Barkan and Sheinin[7] determined the KPFP for several gases using the data of the second-order virial coefficient and transport properties such as viscosity. Avlonitis[8] presented a method for deriving KPFP using second-order virial coefficients compared with the experimental data for nearly perfect gases, i.e., xenon, krypton, methane, ethane, propane, butane, nitrogen, carbon dioxide and hydrogen sulfide. Tohidi[9] using two different methods, reported the KPFP for eight different gases. In the first method, based on the cage occupancy, hydration number of xenon, and dissociation pressure experimental data the KPFP for xenon was found. Then, the xenon was selected as the key component and the KPFP of C1, C2 and C3 were calculated using experimental data on their binary mixtures with xenon. In the second method, the KPFP were derived from the intersections of the plot of σ as a function of ε/k for different structures[9]. Hendriks et al.[10] found that when ethane is present in binary gas mixtures, for example, methane + ethane, a structure transition may be seen especially when the other hydrate former can occupy the smaller cages. Sloan[11]

optimized KPFP for several gases using experimental data. Subramanian et al.[12, 13] reported that there would be a structural transition from sI to sII, when mixtures of methane and ethane form hydrates at 274.2 K and 0.72 and 0.75 mol% of methane. Ballard and Sloan[14] generated the phase diagram of different binary and ternary gas mixtures at 277.6 K by optimizing the system Gibbs free energy. Later, they reported new KPFP based on experimental data and using vdW-P solid solution theory[15]. The results showed that there are multiple phase transition points as a function of temperature when methane composition is between 0.7 to 0.75 mole percent. In 2007, Sloan and Koh[16] reported KPFP for many gases.

During these years, several KPFP are reported using different methods. Applying each set of reported KPFP, different structures can be predicted for a unique gas mixture. An incorrect prediction of the structure causes an incorrect prediction of the hydrate equilibrium conditions. the In this work, first, the KPFP reported in the literature are compared to predict both stable hydrate structure and also gas hydrate dissociation temperature based on this structure. Then, the results of the optimized KPFP for methane, ethane, propane, i-butane, and their mixtures are presented and found highly accurate.

2. THERMODYNAMIC MODEL

The equilibrium state occurs when the chemical potentials are equal in these two phases[16]:

$$\Delta\mu_w^H = \Delta\mu_w^L \qquad (1)$$

where $\Delta\mu_w$ is the difference between water chemical potential in unoccupied and occupied hydrate lattice, and superscripts H and L refer to hydrate and liquid phases, respectively.

The right hand side of Eq. (1) could be estimated by the following expression given by Holder et al.[17]

$$\frac{\Delta\mu_w^L}{RT} = \frac{\Delta\mu_w^\circ}{RT_\circ} - \int_{T_\circ}^{T} \frac{\Delta h_w^L}{RT^2} dT + \int_0^P \frac{\Delta v_w^L}{RT} dP + \ln a_W \tag{2}$$

where Δh_w^L is the difference between water enthalpy in unoccupied hydrate lattice and liquid water which is defined as follows:

$$\Delta h_w^L = \Delta h_w^\circ + \int_{T_\circ}^{T} \Delta C_{pw}^L dT \tag{3}$$

$$\Delta C_{pw}^L = E + F\left(T - 273.15\right) \tag{4}$$

where ΔC_{pw}^L is the difference between water heat capacity in the unoccupied hydrate lattice and liquid water. The parameters *E* and *F* are reported in Table 1. $\Delta\mu_w^\circ$, Δh_w°, and Δv_w^l are differences between the water chemical potential and enthalpy in unoccupied hydrate lattice and liquid water at the reference temperature, and water molar volume in unoccupied hydrate lattice and a liquid water an respectively. These values are reported in Table 2. Parameters *P*, $a_w, T_\circ$ and *R* are system pressure, water activity, the reference temperature (273.15 K), and the universal gas constant, respectively.

Table 1

Table 2

In the absence of any additive such as salts or alcohols in the aqueous phase, the water activity, a_w, can be estimated as follows:

$$a_w = 1 - \sum_{i=1}^{N} x_i^{guest} \tag{5}$$

where solubility of guest compounds in water phase, x_i^{guest}, is calculated using the following equation[18]:

$$x_i^{guest} = \frac{f_i^v}{H_i(T)\exp\left(\frac{Pv}{RT}\right)} \tag{6}$$

where f_i^v, is the fugacity of the guest molecules in the gas phase which is calculated using the Peng-Robinson equation of state[19] (PR EoS) in this work and the values of T_C, P_C and ω are reported in Table 3[20]. H is the Henry constant of each guest molecule, v is the partial molar volume of each guest molecule and T is the system temperature. Henry constant of each guest molecule can be calculated using the following equation[21]:

$$-\ln\left(\frac{H_i(T)}{101325}\right) = H_i^{[1]} + \frac{H_i^{[2]}}{T} + H_i^{[3]}\ln(T) + H_i^{[4]}T \tag{7}$$

where, $H_i^{[1]}$, $H_i^{[2]}$, $H_i^{[3]}$, and $H_i^{[4]}$ are reported in Table 4.

Table 4

The left hand side of Eq. (1), $\Delta\mu_w^H$, can be estimated using the solid solution theory of vdW-P[3]:

$$\Delta\mu_w^H = -RT\sum_{m=1}^{2} v'_m \ln\left(1-\sum_{j}^{nc}\theta_{mj}\right) \tag{8}$$

where υ'_m, is the number of cavities type m to the number of water molecules in a hydrate unit cell, θ_{mj} is the fraction of the type m cavities occupied by the j type guest molecules which is described in the following equation:

$$\theta_{mj} = C_{mj} f_j \Big/ \left(1 + \sum_j^{nc} C_{mj} f_j \right) \tag{9}$$

where C_{mj} is the Langmuir constant which is calculated using the relations given by McKoy and Sinanoglu[4]:

$$C_{mj} = \frac{4\pi}{kT} \int_0^{\infty} \exp\left[-\frac{\omega'(r)}{kT} \right] r^2 dr \tag{10}$$

$$\omega'(r) = 2z\varepsilon \left[\frac{\sigma^{12}}{R'^{11} r} \left(\delta^{10} + \frac{a}{R'} \delta^{11} \right) - \frac{\sigma^6}{R'^5 r} \left(\delta^4 + \frac{a}{R'} \delta^5 \right) \right] \tag{11}$$

$$\delta^N = \frac{1}{N} \left(1 - \frac{r}{R'} - \frac{a}{R'} \right)^{-N} - \left(1 + \frac{r}{R'} - \frac{a}{R'} \right)^{-N} \tag{12}$$

where k is the Boltzmann's constant and $\omega'(\mathrm{r})$ is the cell potential. The Kihara potential parameters a, σ and ε are the hard core radius, the collision diameter and the depth of energy well, respectively, N is a parameter (N=4, 5, 10, 11), z, r and R' are respectively the coordinate number, the radius and the mean cavity radius.

Finally, by combining Eq. (2) and (8), the following equation will be obtained which predicts the hydrate equilibrium condition, T and P:

$$\sum_{m=1}^{2} \upsilon'_m \ln\left(1 + \sum_{j=1}^{nc} C_{mj} f_j \right) = \frac{\Delta \mu_w^{\circ}}{RT_{\circ}} - \int_{T_{\circ}}^{T} \frac{\Delta h_w^l}{RT^2} dT + \int_0^P \frac{\Delta v_w^l}{RT} dP - \ln a_w \tag{13}$$

Different sets of KPFP, a, σ, ε, are reported in the literature. Table 5 shows some of the most popular sets for methane, ethane, propane and i-butane, the main constituents of natural gas.

Table 5

Based on Eq. (13), different sets of Kihara potential parameters may lead to different values of hydrate equilibrium conditions and consequently different structures.

It should be noted that the determination of hydrate structures, especially for gas mixtures, is based on the fact that at a given pressure, the temperatures for the two structures, I and II, are calculated and the structure corresponds to the highest temperature is considered as the stable structure. In some cases, and based on the above criteria, the predicted structure is incorrect, especially for natural gas systems. Consequently, the predicted dissociation condition is also incorrect. In other words, the predicted dissociation temperature for the more stable structure is very different from the experimental values and this shortcoming is due to the inaccuracy of the KPFP in determining the correct conditions.

To overcome these two shortcomings, in this work, the new KPFP are optimized using the genetic algorithm which is described in the following section. This set, by comparison with the literature hydrate data, predicts the hydrate phase boundary and structure precisely.

a. PARAMETERS OPTIMIZATION

Genetic algorithm (GA) was first introduced by Holland[22]. GA is a suitable method for solving problems associated with search and optimization. This algorithm works with a population of "unique members" in which each member has a defined fitness. Members with higher degrees of fitness have more opportunities for "fertility" through "blending" with other members of the population. The new members inherit some of their parent's traits. Members' traits distribute in their populations and the members change due to multiple reproduction and generation of sequential populations. If the algorithm is well-designed, the population will converge to an optimal solution to the problem. The genetic algorithm begins with the

definition of optimization parameters and ends once the convergence condition is satisfied. The adjustable parameters are determined as follows:

a) Chromosome (Optimization parameters) and cost function

Optimization parameters and the cost function must be defined in this algorithm. In the culture of genetics algorithm, a chromosome is a set of optimization parameters as defined in Eq. (14):

$$\text{Chromosome} = [\alpha, \sigma, \varepsilon] \tag{14}$$

α, σ, and ε are optimization parameters that have real numeric values which are described in section 2.1.b.

In optimization problems, the aim is to minimize the cost function known as the objective function (*OF*). In this work, *OF* is calculated using Eq. (15):

$$OF = \Delta er + \Delta er_{\text{total}} \tag{15}$$

For methane and ethane:

$$\Delta er = \sum_{i=1}^{N} \left| T_i^{Exp.} - T_i^{sI} \right| \tag{16}$$

For propane and isobutane:

$$\Delta er = \sum_{i=1}^{N} \left| T_i^{Exp.} - T_i^{sII} \right| \tag{17}$$

and

$$\Delta er_{\text{total}} = \begin{cases} \sum_{i=1}^{N} \left| T_i^{Exp} - T_i^{sI} \right| & if \quad T_{sI} > T_{sII} \\ \sum_{i=1}^{N} \left| T_i^{Exp} - T_i^{sII} \right| & if \quad T_{sII} > T_{sI} \end{cases} \tag{18}$$

Δer is described differently for methane, ethane, propane and isobutane since they form sI and sII, respectively. Δer_{total} is added to the OF, to not let the optimization process go toward the prediction of the wrong structure.

b) Initial population

The initial matrix is created using Eq. (19) noting the allowed range of each parameter:

$$IPOP = (hi - low) \times \text{random}\{N_{ipop}, N_{Par}\} + low \quad (19)$$

N_{ipop} : The number of the initial population

N_{Par} : The number of optimization parameters

$\text{random}\{N_{ipop}, N_{Par}\}$: A function that generates random numbers between zero and one

hi : The maximum value in the allowed range of each parameter

low : The minimum value in the allowed range of each parameter

c) Tournament Selection

The Tournament selection[23] method is used to select parents. The choices of parents are based on an approach that even the weakest chromosomes have a luck to be selected. This approach leads the optimization to find global answers.

d) Mating

Mating is the process of producing two new chromosomes from each selected parent. One of the most common methods of mating is the crossover methods[24]. One or more locations in each chromosome are selected as cutoff-points. By choosing a random point as a cutoff point in the chromosome, the parameters in further that point will be exchanged between each parent [25]. The cutoff-point will be calculated using the BLX-α method[26].

e) Mutation

The mutation rate is calculated using an exponential function in the form of Eq. (20):

$$\mu = \mu_o \, e^{-Counter} \quad (20)$$

μ_o is a primary mutation rate, and *counter* is the number of repetitions performed.

The continuous genetic algorithm works well when the mutation rate is between 1 to 20 percent. If the mutation rate is of over 20 percent, a bunch of good parameters will be lost.

f) Termination

The optimization process will be terminated when the main loop is repeated 100 times. Finally, the chromosome with the highest fitness value will be considered as the optimum value.

---------- optim. check shavad

3. RESULT AND DISCUSSION

The literature hydrate dissociation temperatures for methane, ethane, propane and i-butane are reported in Table 6. A complete set of experimental data is obtained from the literature and 856 data points were found. Using different sets of KPFP reported in Table 5, the average absolute deviation, *AAD*, for hydrate dissociation temperatures are reported in Table 7.

As can be seen, KPFP reported by Holder and Hand[6], Barkan and Sheinin[7], and Avlonitis[8] could not predict the hydrate formation condition precisely.

Table 6

Table 7

The KPFP reported in Table 5 are also used to predict hydrate formation conditions of different mixtures of methane, ethane, propane, and i-butane. The mixtures, depend on their compositions, may form either sI or sII. The hydrate formation structure for each set of data is determined using the thermodynamic model described in section 2. The stable structure is the one with higher hydrate formation temperature and/or lower pressure. Holder and Hand[6], reported experimental hydrate formation data for mixtures of ethane and propane. They also claimed that each set of data will form different structures when thermodynamic conditions are changed. For example, a structural transition is observed for a mixture of 74% mol ethane and

26% mol propane. To justify their statement, all the reported KPFP in Table 5 are applied to that set of data and the results are depicted in Fig. 1.

Figure 1

A closer view of Fig. 1 reveals that some of the reported KPFP could not predict the correct structure. The *AAD* of calculated hydrate formation temperature using the reported KPFP by Parish and Prausnitz[5], Holder and Hand[6], Barkan and Sheinin[7], Avlonitis[8], Tohidi[9], Sloan[11], Sloan and Koh[16], and Hydrafact[1] Software. were 4.69, 14.82, 9.47, 2.67, 0.18, 5.29, 8.07 and 0.15 K, respectively.

Figures 2 and 3 are also shown the equilibrium conditions for 90.4% mol methane and 9.6% mol ethane mixture, and 96.5% mol methane and 3.5% mol propane mixture, respectively.

Figure 2

Figure 3

As shown in the Fig.2, some of the reported KPFP predict the structure I and some the structure II as the correct structure. According to Subramanian et al.[12], the structure II of hydrate is the correct structure for this system. Hence only the KPFP reported by Tohidi[9] have predicted the correct structure, which has the *AAD* of calculated hydrate formation temperature 1.02 K.

According to Figure 3, the parameters reported by Kihara by Parish and Prausnitz[5], Tohidi[9], Sloan[11], Sloan and Koh[16],and Hydrafact Software predicted the correct structure for this gas mixture, but some of them have high *AAD*.

Reported *AAD*s are high in some cases due to the prediction of wrong structures and/or low accuracy of the reported KPFP in prediction of equilibrium conditions. To overcome this

[1] HydraFlash (version 3.6) supplied by Hydrafact Ltd. (UK).

challenge, in this work, new KPFP are optimized for pure gases (methane, ethane, propane and, isobutane) using GA as described in section 2.1. Experimental hydrate formation condition data of pure gases are given in Table 6. Forty percent of the reported experimental data are used in the optimization process. The new optimized KPFP are reported in Table 8.

Table 8

The new optimized KPFP are used in the thermodynamic model and then the hydrate formation condition of pure gases and some of their mixtures are calculated and depicted in Fig. 4. The *AAD* is reported in Table 7.

Figure 4

As can be seen in Table 7, the results of hydrate formation conditions of pure gases and their mixtures using the optimized KPFP showed that the new parameters are more accurate than the former reported parameters except for pure propane and mixtures of ethane and propane.

4. CONCLUSION

In this paper, the van der Waals Platteeuw solid solution theory along with the Peng-Robinson equation of state using different KPFP are applied to predict the hydrate formation conditions of pure methane, ethane, propane, i-butane and also their mixtures. The *AAD* of each set of experimental data using different KPFP are reported. The reported *AAD*s are high in some cases due to the prediction of wrong structures and/ or low accuracy of the reported KPFP. Therefore, new KPFP are optimized for pure methane, ethane, propane and i-butane hydrate experimental data using GA algorithm in Matlab. Then, the optimized KPFP are also used for gas mixtures. The reported results showed that KPFP are highly accurate and also are capable of predicting the correct hydrate structures.

Nomenclature

Roman Characters:

a	Hard core radius, Å
a_w	Water activity
AAD	Average Absolute Deviation, K
C_{mj}	Langmuir constant for component j in cavity m, kPa^{-1}
$\Delta C'_{pw}$	Difference in heat capacity between hydrate lattice and liquid water, J/mol/K
f_i^v	The fugacity of the guest molecules in the gas phase
Δh_w^l	Difference in enthalpy between hydrate lattice and liquid water, J/mol
Δh_w°	Difference in enthalpy between hydrate lattice and liquid water in 273.15 K, J/mol
H_i	Henry constant for component i, Pa^{-1}
$IPOP$	Initial population
k	Boltzmann's constant, J/K
N_{ipop}	The number of initial population
N_{Par}	The number of optimization parameters
P	Pressure, kPa
P_c	Critical pressure, kPa
r	Radius cavity radius, Å
R	Universal gas constant, J/mol/K
R'	Mean cavity radius

T	Temperature, K
T_c	Critical temperature, K
z	Coordinate number

Greek Characters:

ε	Depth of energy well, J
σ	Collision diameter, Å
υ_m'	Number of cavities type *m* to the number of water molecules in a hydrate lattice
ν	Partial molar volume of each guest molecule, cm^3/mol
$\Delta\nu_w^l$	Difference in water molar volume between an empty hydrate lattice and liquid phase, cc/mol
$\Delta\mu_W^H$	Difference in Water chemical potential between an empty hydrate lattice and hydrate, J/mol
$\Delta\mu_W^L$	Difference in Water chemical potential between an empty hydrate lattice and liquid phase, J/mol
$\Delta\mu_w^\circ$	Difference in water chemical potential between hydrate lattice and liquid water at 273.15 K, J/mol
ω	Acentric factor
ω'(r)	Cell potential

Superscripts and Subscripts:

0	Reference state
Calc.	Calculated
Counter	Number of repetitions performed
Exp.	Experiment

H	Hydrate phase
L	Liquid water
w	Water
v	vapor

REFERENCES

[1] M.v. Stackelberg, H. Müller, On the structure of gas hydrates, The Journal of Chemical Physics, 19, (1951), 1319-1320 https://doi.org/10.1063/1.1748038
[2] J.A. Ripmeester, S.T. John, C.I. Ratcliffe, B.M. Powell, A new clathrate hydrate structure, Nature, 325, (1987), 135-136 https://doi.org/10.1038/325135a0
[3] J.v.d. Waals, J. Platteeuw, Clathrate solutions, Advances in chemical physics, (1958), 1-57 https://doi.org/10.1002/9780470143483.ch1
[4] V. McKoy, O. Sinanoğlu, Theory of dissociation pressures of some gas hydrates, The journal of chemical physics, 38, (1963), 2946-2956 https://doi.org/10.1063/1.1733625
[5] W.R. Parrish, J.M. Prausnitz, Dissociation pressures of gas hydrates formed by gas mixtures, Industrial & Engineering Chemistry Process Design and Development, 11, (1972), 26-35 https://doi.org/10.1021/i260041a006
[6] G. Holder, J. Hand, Multiple-phase equilibria in hydrates from methane, ethane, propane and water mixtures, AIChE Journal, 28, (1982), 440-447 https://doi.org/10.1002/aic.690280312
[7] E. Barkan, D. Sheinin, A general technique for the calculation of formation conditions of natural gas hydrates, Fluid phase equilibria, 86, (1993), 111-136 https://doi.org/10.1016/0378-3812(93)87171-V
[8] D. Avlonitis, The determination of Kihara potential parameters from gas hydrate data, Chemical engineering science, 49, (1994), 1161-1173 https://doi.org/10.1016/0009-2509(94)85087-9
[9] B. Tohidi-Kalorazi, Gas hydrate equilibria in the presence of electrolyte solutions, in, Heriot-Watt University, (1995), http://hdl.handle.net/10068/634023
[10] E. Hendriks, B. Edmonds, R. Moorwood, R. Szczepanski, Hydrate structure stability in simple and mixed hydrates, Fluid phase equilibria, 117, (1996), 193-200 https://doi.org/10.1016/0378-3812(95)02953-2
[11] E.D. Sloan Jr, Clathrate Hydrates of Natural Gases, revised and expanded, CRC press, (1998) https://doi.org/10.1021/ja9856194
[12] S. Subramanian, R. Kini, S. Dec, E. Sloan Jr, Evidence of structure II hydrate formation from methane+ ethane mixtures, Chemical Engineering Science, 55, (2000), 1981-1999 https://doi.org/10.1016/S0009-2509(99)00389-9
[13] S. Subramanian, A. Ballard, R. Kini, S. Dec, E. Sloan, Structural transitions in methane+ ethane gas hydrates—Part I: Upper transition point and applications, Chemical Engineering Science, 55, (2000), 5763-5771 https://doi.org/10.1016/S0009-2509(00)00162-7
[14] A. Ballard, E. Sloan Jr, Structural transitions in methane+ ethane gas hydrates—part II: Modeling beyond incipient conditions, Chemical engineering science, 55, (2000), 5773-5782 https://doi.org/10.1016/S0009-2509(00)00163-9
[15] A.L. Ballard, E. Sloan Jr, Optimizing thermodynamic parameters to match methane and ethane structural transition in natural gas hydrate equilibria, Annals of the New York Academy of Sciences, 912, (2000), 702-712 https://doi.org/10.1111/j.1749-6632.2000.tb06826.x
[16] E.D. Sloan Jr, C. Koh, Clathrate hydrates of natural gases, CRC press, (2007) ISBN: 1420008498
[17] G. Holder, G. Corbin, K. Papadopoulos, Thermodynamic and molecular properties of gas hydrates from mixtures containing methane, argon, and krypton, Industrial & Engineering Chemistry Fundamentals, 19, (1980), 282-286 https://doi.org/10.1021/i160075a008

[18] G. Holder, S. Zetts, N. Pradhan, Phase behavior in systems containing clathrate hydrates: a review, Reviews in chemical engineering, 5, (1988), 1-70 https://doi.org/10.1515/REVCE.1988.5.1-4.1
[19] D.-Y. Peng, D.B. Robinson, A new two-constant equation of state, Industrial & Engineering Chemistry Fundamentals, 15, (1976), 59-64 https://doi.org/10.1021/i160057a011
[20] Perry's Chemical engineer's handbook, eighth edition, assistant editor, New York : McGraw-Hill, (2007) ISBN-10: 0071422943
[21] J.B. Klauda, S.I. Sandler, A fugacity model for gas hydrate phase equilibria, Industrial & engineering chemistry research, 39, (2000), 3377-3386 https://doi.org/10.1021/ie000322b
[22] J. Holland, Adaptation in natural and artificial systems, univ. of mich. press, Ann Arbor, (1975), https://doi.org/10.1137/1018105
[23] B.L. Miller, D.E. Goldberg, Genetic algorithms, tournament selection, and the effects of noise, Complex systems, 9, (1995), 193-212
[24] A.H. Wright, Genetic algorithms for real parameter optimization, in: Foundations of genetic algorithms, Elsevier, (1991), pp. 205-218 https://doi.org/10.1016/B978-0-08-050684-5.50016-1
[25] Z. Michalewicz, Genetic algorithms+ data structures= evolution programs, Springer Science & Business Media, (2013) https://doi.org/10.1007/978-3-662-03315-9
[26] L.J. Eshelman, J.D. Schaffer, Real-coded genetic algorithms and interval-schemata, in: Foundations of genetic algorithms, Elsevier, (1993), pp. 187-202 https://doi.org/10.1016/B978-0-08-094832-4.50018-0
[27] W. Deaton, E. Frost Jr, Gas hydrates and their relation to the operation of natural-gas pipe lines, in, Bureau of Mines, Amarillo, TX (USA). Helium Research Center, (1946),
[28] R. Kobayashi, D.L. Katz, Methane hydrate at high pressure, Journal of Petroleum Technology, 1, (1949), 66-70 https://doi.org/10.2118/949066-G
[29] H.O. McLeod Jr, J.M. Campbell, Natural gas hydrates at pressures to 10,000 psia, Journal of Petroleum Technology, 13, (1961), 590-594 https://doi.org/10.2118/1566-G-PA
[30] D.R. Marshall, S. Saito, R. Kobayashi, Hydrates at high pressures: Part I. Methane-water, argon-water, and nitrogen-water systems, AIChE Journal, 10, (1964), 202-205 https://doi.org/10.1002/aic.690100214
[31] J. Jhaveri, D.B. Robinson, Hydrates in the methane-nitrogen system, The Canadian Journal of Chemical Engineering, 43, (1965), 75-78 https://doi.org/10.1002/cjce.5450430207
[32] T.J. Galloway, W. Ruska, P.S. Chappelear, R. Kobayashi, Experimental measurement of hydrate numbers for methane and ethane and comparison with theoretical values, Industrial & Engineering Chemistry Fundamentals, 9, (1970), 237-243 https://doi.org/10.1021/i160034a008
[33] V.K. Verma, Gas hydrates from liquid hydrocarbon-water systems, in, University of Michigan, (1974),
[34] B.J. Falabella, M. Vanpee, Experimental determination of gas hydrate equilibrium below the ice point, Industrial & Engineering Chemistry Fundamentals, 13, (1974), 228-231 https://doi.org/10.1021/i160051a012
[35] J. De Roo, C. Peters, R. Lichtenthaler, G. Diepen, Occurrence of methane hydrate in saturated and unsaturated solutions of sodium chloride and water in dependence of temperature and pressure, AIChE Journal, 29, (1983), 651-657 https://doi.org/10.1002/aic.690290420
[36] J.L. Thakore, G.D. Holder, Solid vapor azeotropes in hydrate-forming systems, Industrial & Engineering Chemistry Research, 26, (1987), 462-469 https://doi.org/10.1021/ie00063a011

[37] K.Y. Song, R. Kobayashi, Final hydrate stability conditions of a methane and propane mixture in the presence of pure water and aqueous solutions of methanol and ethylene glycol, Fluid phase equilibria, 47, (1989), 295-308 https://doi.org/10.1016/0378-3812(89)80181-5
[38] S. Adisasmito, R.J. Frank III, E.D. Sloan Jr, Hydrates of carbon dioxide and methane mixtures, Journal of Chemical and Engineering Data, 36, (1991), 68-71 https://doi.org/10.1021/je00007a020
[39] Y. Deng, Xu, X., Zhang, L., A Primary Study on Composition of Methane Hydrate, in: Permafrost Sixth International Conference, Beijing, China, (1993),
[40] G.R. Dickens, M.S. Quinby-Hunt, Methane hydrate stability in seawater, Geophysical Research Letters, 21, (1994), 2115-2118 https://doi.org/10.1029/94GL01858
[41] T.Y. Makogon, E.D.J. Sloan, Phase equilibrium for methane hydrate from 190 to 262 K, Journal of Chemical and Engineering Data, 39, (1994), 351-353 https://doi.org/10.1021/je00014a035
[42] U. Hütz, P. Englezos, Measurement of structure H hydrate phase equilibrium and the effect of electrolytes, Fluid phase equilibria, 117, (1996), 178-185 https://doi.org/10.1016/0378-3812(95)02951-6
[43] D.-H. Mei, J. Liao, J.-T. Yang, T.-M. Guo, Experimental and modeling studies on the hydrate formation of a methane+ nitrogen gas mixture in the presence of aqueous electrolyte solutions, Industrial & engineering chemistry research, 35, (1996), 4342-4347 https://doi.org/10.1021/ie9601662
[44] T. Komai, Y. Yamamoto, S. Ikegami, Equilibrium properties and kinetics of methane and carbon dioxide gas hydrate formation/dissociation, ACS Division of Fuel Chemistry, Preprints, 42, (1997), 568-570
[45] T. Komai, Y. Yamamoto, Equilibrium properties and kinetics of methane and carbon dioxide gas hydrate formation/dissociation, in: Abstracts of Papers of the American Chemical Society, AMER CHEMICAL SOC 1155 16TH ST, NW, WASHINGTON, DC 20036, (1997), pp. 90-FUEL
[46] J. Nixdorf, L.R. Oellrich, Experimental determination of hydrate equilibrium conditions for pure gases, binary and ternary mixtures and natural gases, Fluid Phase Equilibria, 139, (1997), 325-333 https://doi.org/10.1016/S0378-3812(97)00141-6
[47] E.A. Smelik, H. King, Crystal-growth studies of natural gas clathrate hydrates using a pressurized optical cell, American Mineralogist, 82, (1997), 88-98 https://doi.org/10.2138/am-1997-1-211
[48] S. Nakano, M. Moritoki, K. Ohgaki, High-pressure phase equilibrium and Raman microprobe spectroscopic studies on the methane hydrate system, Journal of Chemical & Engineering Data, 44, (1999), 254-257 https://doi.org/10.1021/je980152y
[49] M. Clarke, P.R. Bishnoi, Determination of the activation energy and intrinsic rate constant of methane gas hydrate decomposition, The Canadian Journal of Chemical Engineering, 79, (2001), 143-147 https://doi.org/10.1002/cjce.5450790122
[50] M.D. Jager, High Pressure Studies of Hydrate Phase Inhibition Using Raman Spectroscopy, in: Ph.D. Chemical Engineering Thesis, Colorado School of Mines, Golden, Colorado, USA, (2001),
[51] S. Yang, S. Cho, H. Lee, C. Lee, Measurement and prediction of phase equilibria for water+ methane in hydrate forming conditions, Fluid Phase Equilibria, 185, (2001), 53-63 https://doi.org/10.1016/S0378-3812(01)00456-3
[52] T. Nakamura, T. Makino, T. Sugahara, K. Ohgaki, Stability boundaries of gas hydrates helped by methane—structure-H hydrates of methylcyclohexane and cis-1, 2-dimethylcyclohexane, Chemical engineering science, 58, (2003), 269-273 https://doi.org/10.1016/S0009-2509(02)00518-3

[53] A.H. Mohammadi, R. Anderson, B. Tohidi, Carbon monoxide clathrate hydrates: equilibrium data and thermodynamic modeling, AIChE journal, 51, (2005), 2825-2833 https://doi.org/10.1002/aic.10526
[54] P. Gayet, C. Dicharry, G. Marion, A. Graciaa, J. Lachaise, A. Nesterov, Experimental determination of methane hydrate dissociation curve up to 55 MPa by using a small amount of surfactant as hydrate promoter, Chemical engineering science, 60, (2005), 5751-5758 https://doi.org/10.1016/j.ces.2005.04.069
[55] O. Roberts, E. Brownscombe, L. Howe, H. Ramser, Constitution diagrams and composition of methane and ethane hydrates, Oil Gas J, 39, (1940), 37-43
[56] H. Reamer, F. Selleck, B. Sage, Some properties of mixed paraffinic and olefinic hydrates, Journal of Petroleum Technology, 4, (1952), 197-202 https://doi.org/10.2118/952197-G
[57] G. Holder, G. Grigoriou, Hydrate dissociation pressures of (methane+ ethane+ water) existence of a locus of minimum pressures, The Journal of Chemical Thermodynamics, 12, (1980), 1093-1104 https://doi.org/10.1016/0021-9614(80)90166-4
[58] H.-J. Ng, D.B. Robinson, Hydrate formation in systems containing methane, ethane, propane, carbon dioxide or hydrogen sulfide in the presence of methanol, Fluid Phase Equilibria, 21, (1985), 145-155 https://doi.org/10.1016/0378-3812(85)90065-2
[59] D. Avlonitis, Multiphase equilibria in oil-water hydrate forming systems, Mémoire de, (1988),
[60] P. Englezos, P. Bishnoi, Experimental study on the equilibrium ethane hydrate formation conditions in aqueous electrolyte solutions, Industrial & Engineering Chemistry Research, 30, (1991), 1655-1659 https://doi.org/10.1021/ie00055a038
[61] S. Nakano, K. Yamamoto, K. Ohgaki, Natural gas exploitation by carbon dioxide from gas hydrate fields—high-pressure phase equilibrium for an ethane hydrate system, Proceedings of the Institution of Mechanical Engineers, Part A: Journal of Power and Energy, 212, (1998), 159-163 https://doi.org/10.1243/0957650981536826
[62] M. Clarke, P. Bishnoi, Determination of the intrinsic rate of ethane gas hydrate decomposition, Chemical Engineering Science, 55, (2000), 4869-4883 https://doi.org/10.1016/S0009-2509(00)00137-8
[63] K. Morita, S. Nakano, K. Ohgaki, Structure and stability of ethane hydrate crystal, Fluid Phase Equilibria, 169, (2000), 167-175 https://doi.org/10.1016/S0378-3812(00)00320-4
[64] E. Larionov, Y.A. Dyadin, F. Zhurko, A.Y. Manakov, Phase Diagrams of the Ternary Gas Hydrate Forming Systems at High Pressures. Part II. Ethane–Methane–Water System, Journal of inclusion phenomena and macrocyclic chemistry, 56, (2006), 303-308 https://doi.org/10.1007/s10847-005-9039-0
[65] W.I. Wilcox, D. Carson, D. Katz, Natural gas hydrates, Industrial & Engineering Chemistry, 33, (1941), 662-665 https://doi.org/10.1021/ie50377a027
[66] B. Miller, E. Strong, Hydrate storage of natural gas, American Gas Association Monthly, 28, (1946), 63-67
[67] D. Robinson, B. Metha, Hydrates in the propanecarbon dioxide-water system, Journal of Canadian Petroleum Technology, 10, (1971), https://doi.org/10.2118/71-01-04
[68] H. Kubota, K. Shimizu, Y. Tanaka, T. MakIta, Thermodynamic properties of R13 (CCIF3), R23 (CHF3), R152a (C2H4F2), and propane hydrates for desalination of sea water, Journal of chemical engineering of Japan, 17, (1984), 423-429 https://doi.org/10.1252/jcej.17.423
[69] S.L. Patil, Measurement of multiphase gas hydrate phase equilibria: Effect of inhibitors and heavier hydrocarbon components, in, University of Alaska, Fairbanks, (1987),

[70] M. Mooijer-van den Heuvel, C. Peters, J. de Swaan Arons, Gas hydrate phase equilibria for propane in the presence of additive components, Fluid phase equilibria, 193, (2002), 245-259 https://doi.org/10.1016/S0378-3812(01)00757-9
[71] O.S. Rouher, A.J. Barduhn, Hydrates of iso-and normal butane and their mixtures, Desalination, 6, (1969), 57-73 https://doi.org/10.1016/S0011-9164(00)80011-9
[72] B.-J. Wu, D.B. Robinson, H.-J. Ng, Three-and four-phase hydrate forming conditions in methane+ isobutane+ water, The Journal of Chemical Thermodynamics, 8, (1976), 461-469 https://doi.org/10.1016/0021-9614(76)90067-7
[73] C.O. Zerpa, P.B. Dharmawardhana, W.R. Parrish, E.D. Sloan, Solubility of cyclopropane in aqueous solutions of potassium chloride, Journal of Chemical and Engineering Data, 24, (1979), 26-28 https://doi.org/10.1021/je60080a006
[74] D.-H. Mei, J. Liao, J.-T. Yang, T.-M. Guo, Hydrate formation of a synthetic natural gas mixture in aqueous solutions containing electrolyte, methanol, and (electrolyte+ methanol), Journal of Chemical & Engineering Data, 43, (1998), 178-182 https://doi.org/10.1021/je9701745

List of Tables

Table1. *E* and *F* values used by other researchers to calculate the specific heat capacity by equation 4.

E (J/mol/K)	*F* (J/mol/K)	Ref.
-38.1162	0.1406	Parrish and Prausnitz[5]
-38.1162	0.1406	Holder and Hand[6]
-38.1200	0.1410	Barkan and Sheinin[7]
-37.8850	0.1770	Avlonitis[8]
-37.8850	0.1770	Tohidi[9]
-38.1200	0.1410	Sloan[11]
-38.1200	0.1410	Sloan and Koh[16]
-38.1200	0.1410	Values used in this work

Table 2. The thermodynamic properties used by other researchers to calculate the difference in the chemical potential of water in the aqueous phase.

Structure I			Structure II			Ref.
Δv_w^l (cc/mol)	Δh_w° (J/mol)	$\Delta \mu_w^\circ$ (J/mol)	Δv_w^l (cc/mol)	Δh_w° (J/mol)	$\Delta \mu_w^\circ$ (J/mol)	
4.6	-4858.0	1264.0	5	-5202.0	882.80	Parrish and Prausnitz[5]
4.6	-5627.0	1155.0	5	-6008.0	883.00	Holder and Hand[6]
4.6	-4616.0	1297.0	5	-5226.0	975.00	Barkan and Sheinin[7]
4.6	-4622.0	1297.0	5	-4986.0	937.00	Avlonitis[8]
4.6	-4622.0	1297.0	5	-4986.0	937.00	Tohidi[9]
4.6	-4622.0	1263.0	5	-4986.0	883.80	Sloan[11]
4.6	-4858.9	1263.6	5	-5202.2	882.80	Sloan and Koh[16]
4.6	-4858.9	1263.6	5	-5202.2	882.80	This work

Δv_w^l: Difference in water molar volume between an empty hydrate lattice and liquid phase, cc/mol. Δh_w°: Difference in water enthalpy between hydrate lattice and liquid water in 273.15 K, J/mol. $\Delta \mu_w^\circ$: Difference in water chemical potential between hydrate lattice and liquid water in 273.15 K, J/mol

Table 3. T_C, P_C and ω of the hydrate formers used in PR EoS [20].

Compound	Tc (K)	P_C (MPa)	ω
C1	190.81	4.595	0.011
C2	305.3	4.872	0.099
C3	369.8	4.301	0.152
iC4	408.14	3.648	0.177

Table 4. Henry Law Constants in equation 7 [21].

Compound	$H_i^{[1]}$	$H_i^{[2]}$	$H_i^{[3]}$	$H_i^{[4]}$
C1	-183.7860	9112.582	25.0405	-0.00015
C2	-268.4410	13369.400	37.5561	-0.00230
C3	-316.4900	15922.700	44.3285	0.00000
iC4	96.1158	-2472.570	-17.3680	0.00000

Table 5. Kihara potential function parameters of gas-water interaction.

Compound	a (Å)	σ (Å)	$\frac{\varepsilon}{k}$ (K)	Ref.
C_1	0.3000	3.2398	153.170	Parrish and Prausnitz[5]
C_2	0.4000	3.3180	174.970	
C_3	0.6800	3.3030	200.940	
iC_4	0.8000	3.1244	220.52	
C_1	0.3330	3.1880	150.730	Holder and Hand[6]
C_2	0.5580	3.1550	174.770	
C_3	0.6460	3.3200	209.020	
iC_4	-	-	-	
C_1	0.3690	3.2078	150.180	Barkan and Sheinin[7]
C_2	0.6760	3.1383	190.800	
C_3	0.8340	3.1440	194.550	
iC_4	0.9590	3.3057	177.290	
C_1	0.3930	3.2500	153.800	Avlonitis[8]
C_2	0.4980	3.4300	184.100	
C_3	0.7640	3.2590	203.300	
iC_4	0.7980	3.0770	231.600	
C_1	0.2950	3.2512	153.690	Tohidi[9]
C_2	0.4880	3.4315	183.320	
C_3	0.7300	3.4900	189.270	
iC_4	0.7980	3.6000	209.580	
C_1	0.3834	3.1439	155.593	Sloan[11]
C_2	0.5651	3.2469	188.181	
C_3	0.6502	3.3093	203.310	
iC_4	0.8706	3.0822	225.160	
C_1	0.3834	3.1439	155.593	Sloan and Koh[16]
C_2	0.5651	3.2469	188.181	
C_3	0.6502	3.4167	192.855	
iC_4	0.8706	3.41691	198.333	

a : Hard core radius, Å. σ: Collision diameter, Å. ε: Depth of energy well, J.

k: Boltzmann's constant, J/K.

Table 6. The experimental data used for pure and mixed gases.

Comp.	No. of data points	Pres. range (MPa)	Ref.
C_1	261	2 – 250	Deaton et al.[27]; Kobayashi et al.[28]; McLeod et al.[29]; Marshall et al.[30]; Jhaveri and Robinson[31]; Galloway et al.[32]; Verma[33]; Falabella et al.[34]; De Roo et al.[35]; Thakore and Holder[36]; Song et al.[37]; Adisasmito et al.[38]; Deng et al.[39]; Dickens et al.[40]; Makogon et al.[41]; Hutz et al.[42]; Mei et al.[43]; Komai et al.[44, 45]; Nixdorf and Oellrich[46]; smelik et al.[47]; Nakano et al.[48]; Clarke et al.[49]; Jager[50]; Yang et al.[51]; Kharrat et al. (2003); Nakamura et al.[52]; Mohammadi et al.[53]; Gayeta et al.[54];
C_2	158	0.40 – 120	Roberts et al.[55]; Deaton et al.[27]; Reamer et al.[56]; Galloway et al.[32]; Falabella et al.[34]; Holder et al.[57]; Holder and Hand[6]; Ng and Robinson[58]; Avlonitis[59]; Englezos et al.[60]; Nixdorf and Oellrich[46]; Nakano et al.[61]; Clarke et al.[62]; Morita et al.[63]; Larionov et al.[64];
C_3	89	0.17 – 10	Wilcox et al. [65]; Miller and Strong [66]; Deaton and Frost [27]; Reamer et al. [56]; Robinson and Metha[67]; Verma [33]; Kubota et al. [68]; Thakore and Holder [36]; Patil [69]; Mooijer-van den Heuvel et al.[70]
iC_4	31	0.10 - 0.17	Sloan and Koh[16], Rouher and Barduhn[71], Thakore and Holder[36].
$C_1 + C_2$	55	0.94 – 68	Deaton and Frost[27], Holder and Grigoriou[57], McLeod and Campbell[29], Holder and Hand[6]
$C_1 + C_3$	69	0.26 – 69	Deaton and Frost[27], Holder and Hand[6], McLeod and Campbell[29], Verma[33], Song and Kobayashi[37], Nixdorf and Oellrich[46]
$C_1 + iC_4$	100	0.30 – 63	Deaton and Frost[27], McLeod and Campbell[29], Wu et al.[72], Ng and Robinson[58]
$C_2 + C_3$	67	0.44 – 2	Holder and Hand[6], Nixdorf and Oellrich[46]
$C_1 + C_2 + C_3$	18	0.92 – 24	Zerpa et al.[73], Nixdorf and Oellrich[46]
$C_1+C_2+C_3+iC_4$	8	0.92 – 3	Mei et al.[74]

Table 7. The Average Absolute Deviation between the experimental and predicted hydrate dissociation conditions for the different Kihara potential function parameters reported by other researchers.

Compound	AAD^* (K)										AAD_{total} (K)
	C_1	C_2	C_3	iC_4	$C_1 + C_2$	$C_1 + C_3$	$C_1 + iC_4$	$C_2 + C_3$	$C_1 + C_2 + C_3$	$C_1+C_2+C_3+iC_4$	
Parrish and Prausnitz[5]	0.38	2.83	0.35	0.08	1.22	1.01	1.11	4.21	2.41	2.98	1.38
Holder and Hand[6]	3.38	3.22	2.70	-	3.78	7.36	-	8.50	4.95	-	3.51
Barkan and Sheinin[7]	2.99	9.60	5.03	5.67	2.29	1.57	3.67	13.36	4.15	8.72	5.33
Avlonitis[8]	1.66	0.69	1.91	1.59	1.00	4.16	6.86	2.56	1.80	6.86	2.39
Tohidi[9]	0.78	0.53	0.35	0.12	0.60	7.37	2.99	0.26	0.90	0.52	1.40
Sloan[11]	0.46	0.75	0.85	2.36	1.13	1.93	3.56	4.86	2.78	2.41	1.56
Sloan and Koh[16]	0.33	8.25	0.21	3.23	4.56	0.76	1.23	6.80	5.75	0.33	2.92
Hydrafact Software	0.30	0.43	0.20	0.11	0.52	0.55	2.73	0.20	0.32	2.34	0.64
This work	0.31	0.43	0.34	0.07	0.39	0.75	1.01	0.32	0.32	0.33	0.45

$^* AAD = \frac{1}{N}\sum_{i=1}^{N}\left|T_{i,Calc.} - T_{i,Exp.}\right|$

Table 8. The values of KPFP optimized in this work..

Hydrate former	a (Å)	σ (Å)	$\frac{\varepsilon}{k}$ (K)
C_1	0.3830	3.14360	155.800
C_2	0.5900	3.29980	178.709
C_3	0.6470	3.41900	191.855
iC_4	0.8921	3.20691	198.332

Figures Captions:

Figures 1. Hydrate dissociation conditions of 74 mole % C_2 + 26 mole % C_3 using Kihara Potential function parameters reported by: **a)** Parrish and Prausnitz[5] **b)** Holder and Hand[6] **c)** Barkan and Sheinin[7] **d)** Avlonitis[8] **e)** Tohidi[9] **f)** Sloan[11] **g)** Sloan and Koh[16] **h)** Hydrafact Software.

Figures 2. Hydrate dissociation conditions of 90.4 mole % C_1 + 9.6 mole % C_2 using Kihara Potential function parameters reported by: **a)** Parrish and Prausnitz[5] **b)** Holder and Hand[6] **c)** Barkan and Sheinin[7] **d)** Avlonitis[8] **e)** Tohidi[9] **f)** Sloan[11] **g)** Sloan and Koh[16] **h)** Hydrafact Software.

Figures 3. Hydrate dissociation conditions of 96.5 mole % C_1 + 3.5 mole % C_3 using Kihara Potential function parameters reported by: **a)** Parrish and Prausnitz[5] **b)** Holder and Hand[6] **c)** Barkan and Sheinin[7] **d)** Avlonitis[8] **e)** Tohidi[9] **f)** Sloan[11] **g)** Sloan and Koh[16] **h)** Hydrafact Software.

Figure 4. Hydrate dissociation conditions of different gas mixtures predicted using Kihara Potential function parameters optimized in this work: **a)** 97.8 mole % C_1 + 2.2 mole % C_2, **b)** 17.7 mole % C_1 + 82.3 mole % C_2, **c)** 74 mole % C_2 + 26 mole % C_3, **d)** 85.15 mole % C_2 + 14.85 mole % C_3, **e)** 96.5 mole % C_1 + 3.5 mole % C_3, **f)** 88.13 mole % C_1 + 11.87 mole % C_3, **g)** 8.7 mole % C_1 + 91.3 mole % iC_4, **h)** 84.52 mole % C_1 + 12.55 mole % C_2 + 2.93 mole % C_3, **i)** 70.5 mole % C_2 + 17.4 mole % C_1 + 12.1 mole % C_3, **j)** 97.25 mole % C_1 + 1.42 mole % C_2 + 1.08 mole % C_3 + 0.25 mole % iC_4.

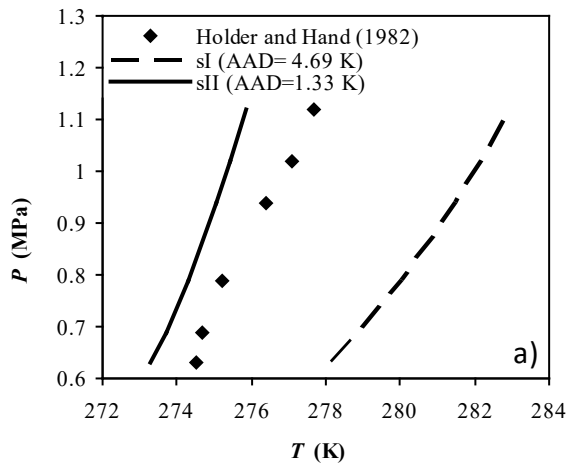
Holder and Hand (1982)
sI (AAD= 4.69 K)
sII (AAD=1.33 K)
P (MPa)
T (K)
a)

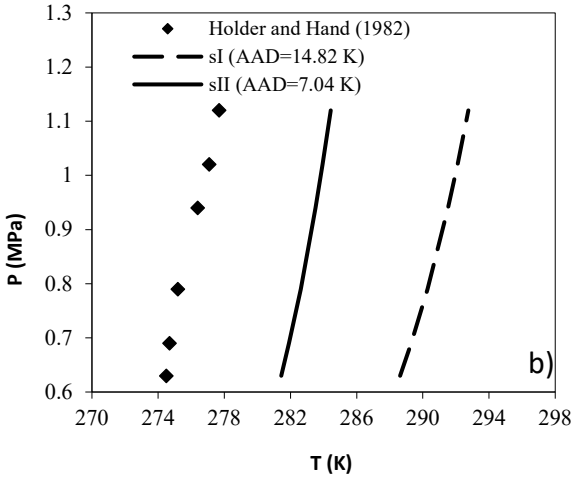
Holder and Hand (1982)
sI (AAD=14.82 K)
sII (AAD=7.04 K)
P (MPa)
T (K)
b)

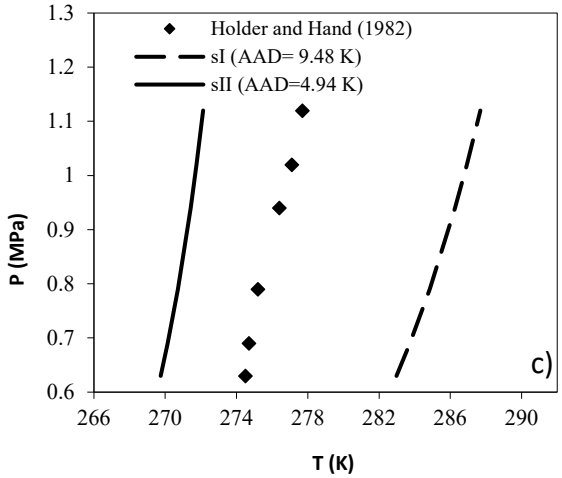
Holder and Hand (1982)
sI (AAD= 9.48 K)
sII (AAD=4.94 K)
P (MPa)
T (K)
c)

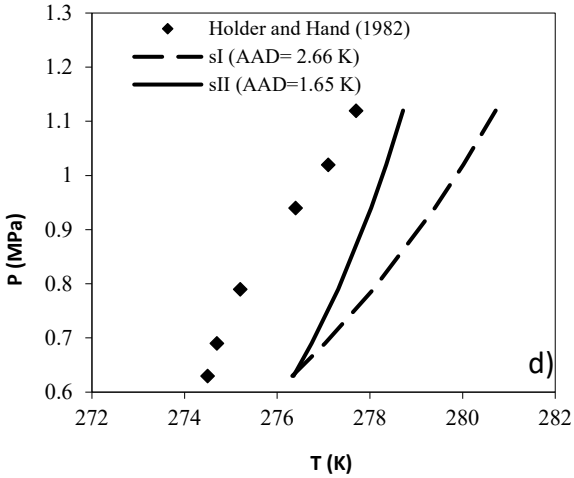
Holder and Hand (1982)
sI (AAD= 2.66 K)
sII (AAD=1.65 K)
P (MPa)
T (K)
d)

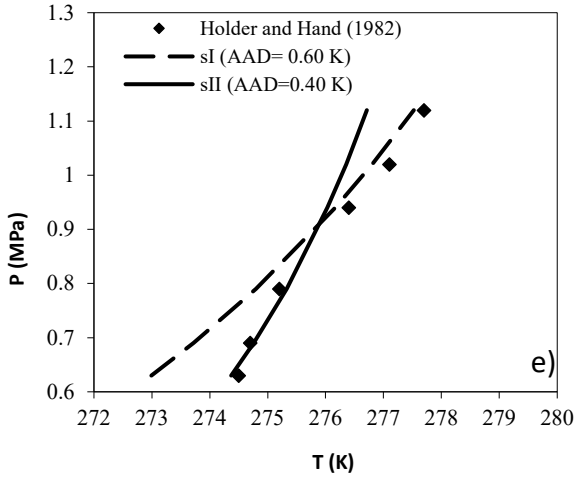
Holder and Hand (1982)
sI (AAD= 0.60 K)
sII (AAD=0.40 K)
P (MPa)
T (K)
e)

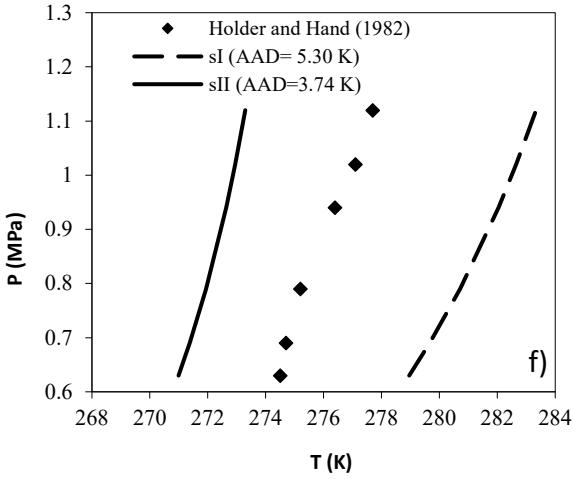
Holder and Hand (1982)
sI (AAD= 5.30 K)
sII (AAD=3.74 K)
P (MPa)
T (K)
f)

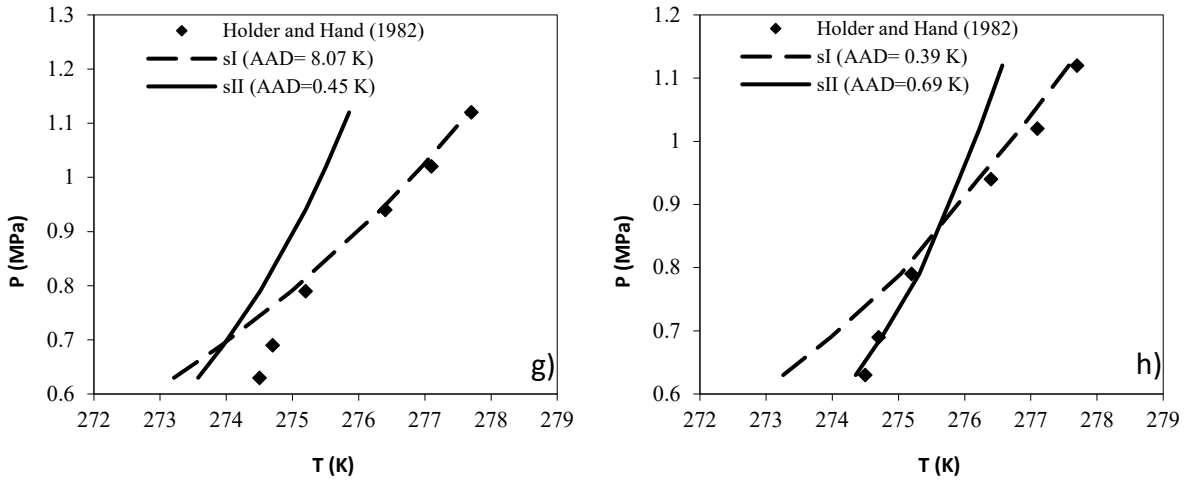

Figure 1. Hydrate dissociation conditions of 74 mole % C_2 + 26 mole % C_3 using Kihara potential function parameters reported by: **a)** Parrish and Prausnitz[5] **b)** Holder and Hand[6] **c)** Barkan and Sheinin[7] **d)** Avlonitis[8] **e)** Tohidi[9] **f)** Sloan[11] **g)** Sloan and Koh[16] **h)** HydraFact Software.

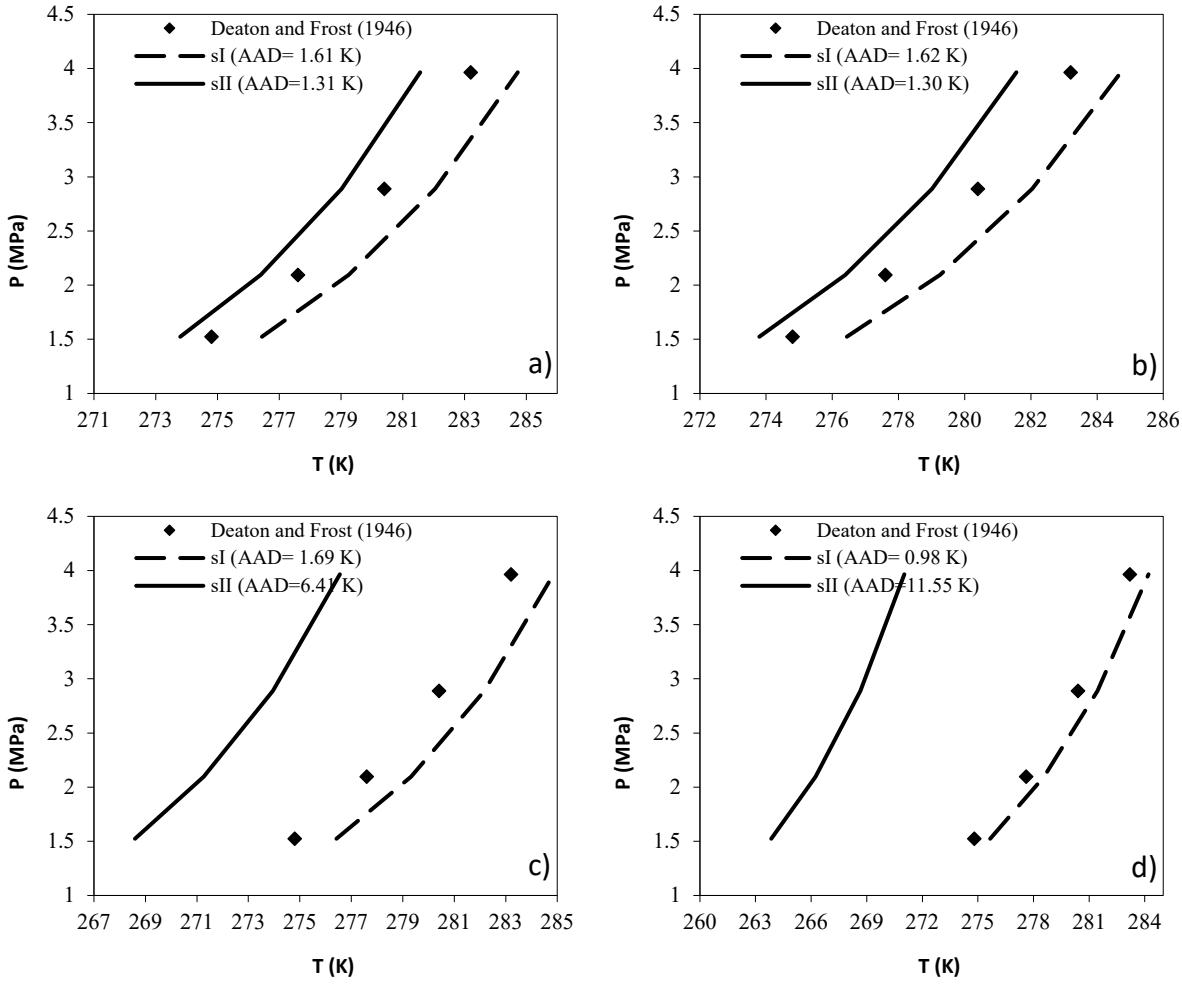
Deaton and Frost (1946)
sI (AAD= 1.61 K)
sII (AAD=1.31 K)
a)
P (MPa)
T (K)
Deaton and Frost (1946)
sI (AAD= 1.62 K)
sII (AAD=1.30 K)
b)
P (MPa)
T (K)
Deaton and Frost (1946)
sI (AAD= 1.69 K)
sII (AAD=6.41 K)
c)
P (MPa)
T (K)
Deaton and Frost (1946)
sI (AAD= 0.98 K)
sII (AAD=11.55 K)
d)
P (MPa)
T (K)

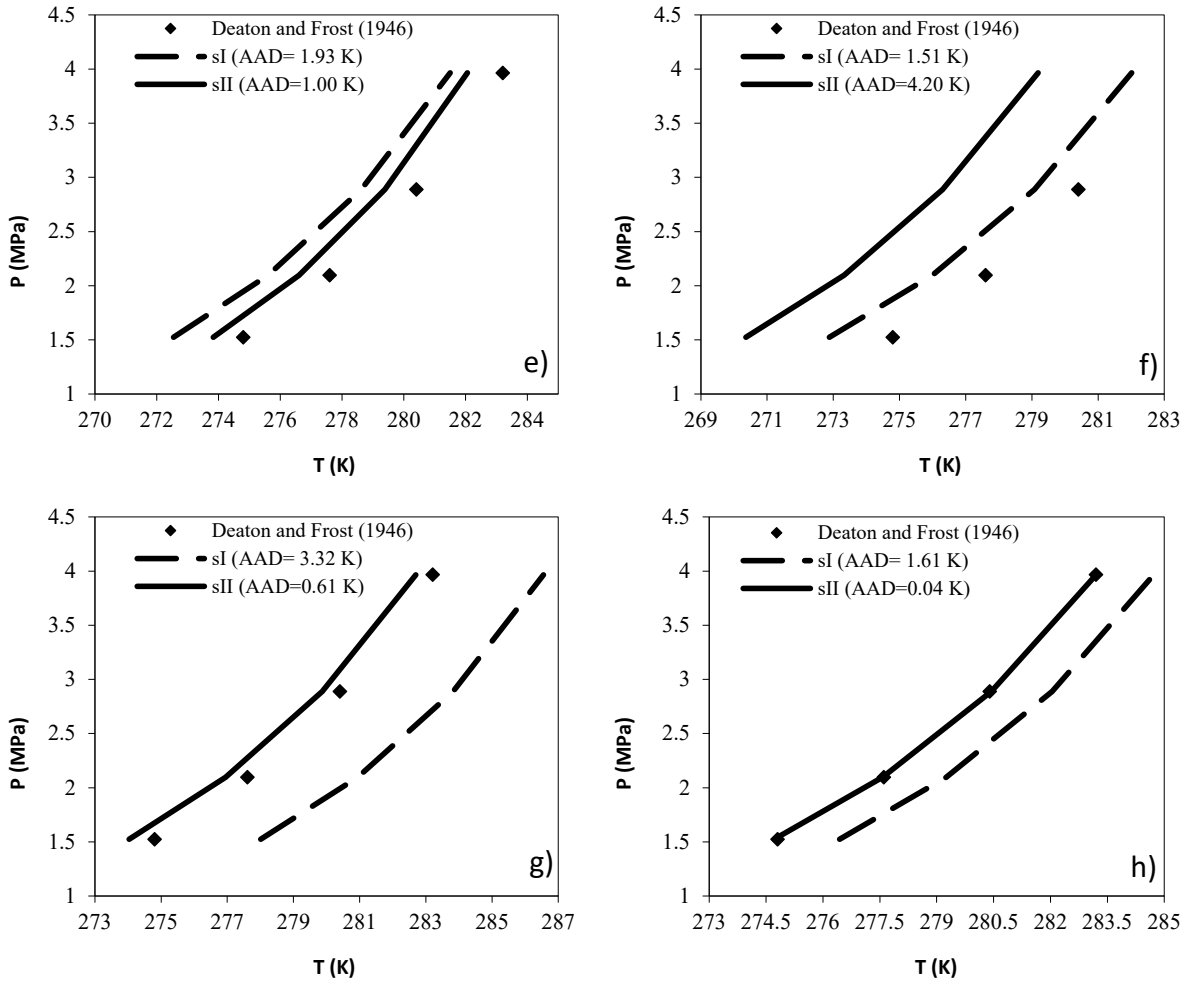

Figure 2. Hydrate dissociation conditions of 74 mole % C_2 + 26 mole % C_3 using Kihara potential function parameters reported by: **a)** Parrish and Prausnitz[5] **b)** Holder and Hand[6] **c)** Barkan and Sheinin[7] **d)** Avlonitis[8] **e)** Tohidi[9] **f)** Sloan[11] **g)** Sloan and Koh[16] **h)** Hydrafact Software.

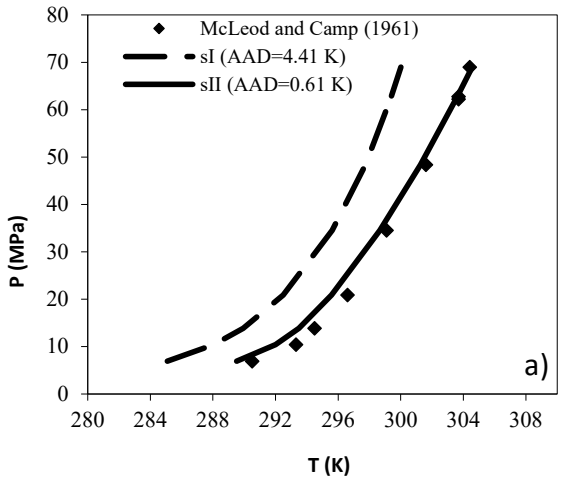
McLeod and Camp (1961)
sI (AAD=4.41 K)
sII (AAD=0.61 K)
a)
P (MPa)
T (K)

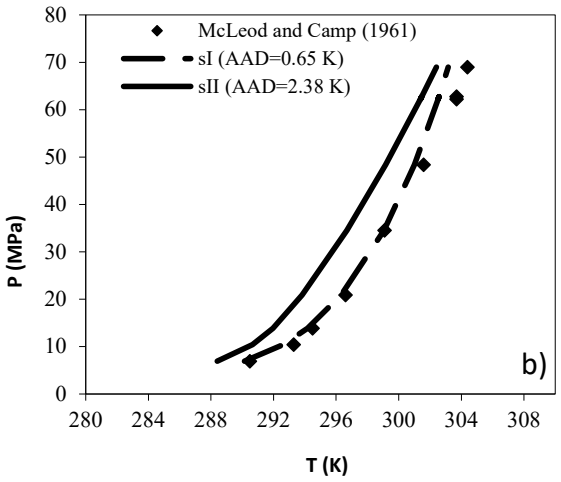
McLeod and Camp (1961)
sI (AAD=0.65 K)
sII (AAD=2.38 K)
b)
P (MPa)
T (K)

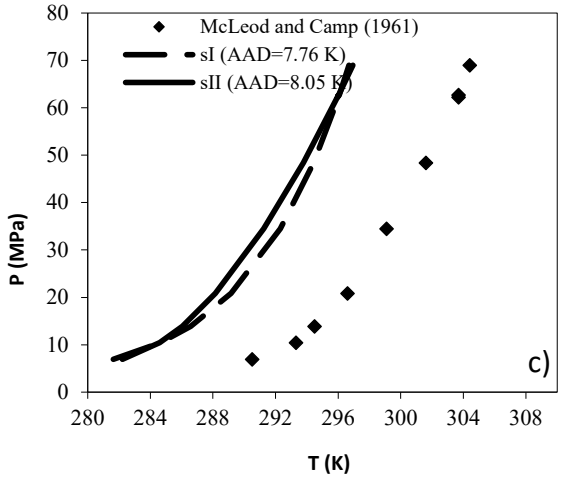
McLeod and Camp (1961)
sI (AAD=7.76 K)
sII (AAD=8.05 K)
c)
P (MPa)
T (K)

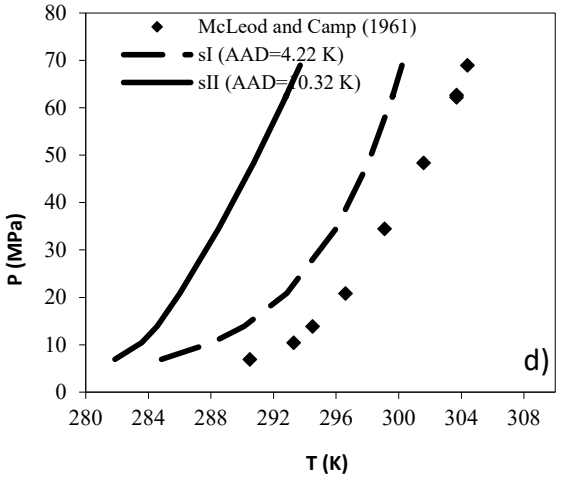
McLeod and Camp (1961)
sI (AAD=4.22 K)
sII (AAD=10.32 K)
d)
P (MPa)
T (K)

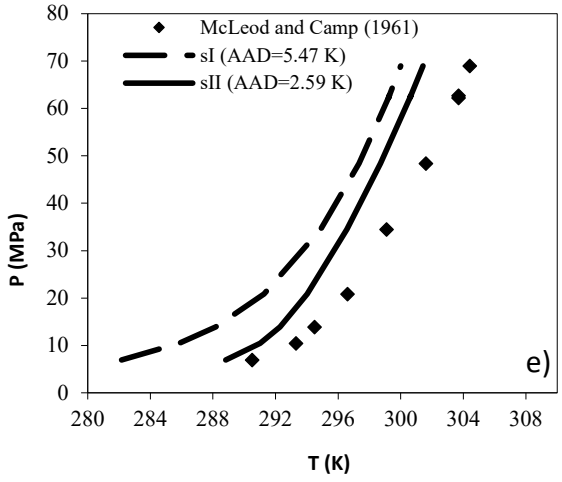
McLeod and Camp (1961)
sI (AAD=5.47 K)
sII (AAD=2.59 K)
e)
P (MPa)
T (K)

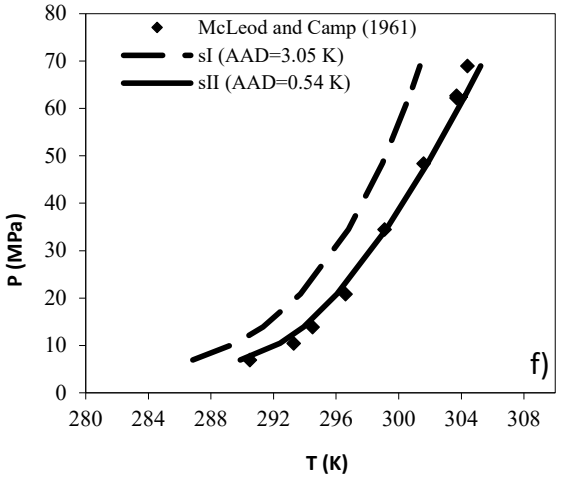
McLeod and Camp (1961)
sI (AAD=3.05 K)
sII (AAD=0.54 K)
f)
P (MPa)
T (K)

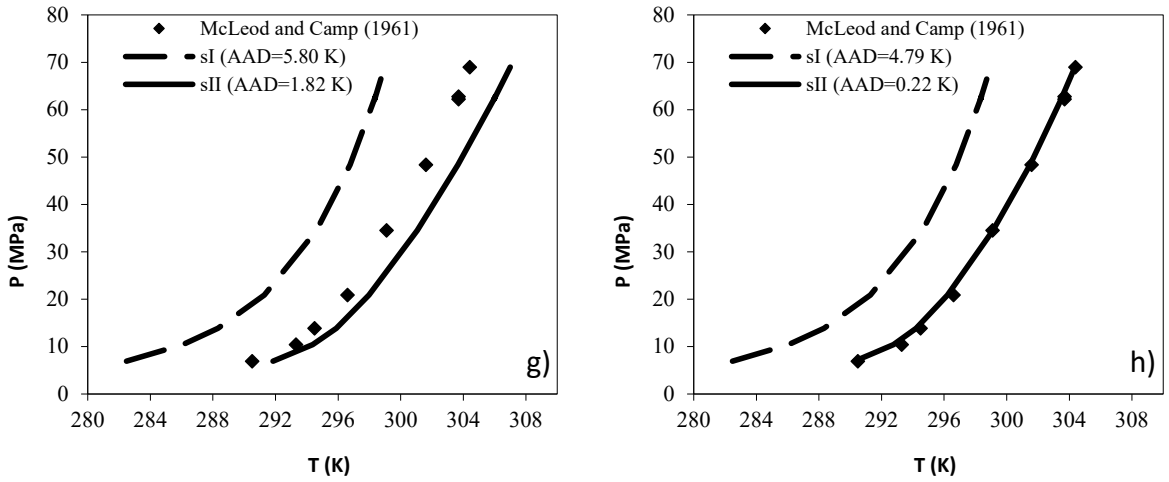

Figure 3. Hydrate dissociation conditions of 96.5 mole % C_1 + 3.5 mole % C_3 using Kihara potential function parameters reported by: **a)** Parrish and Prausnitz[5] **b)** Holder and Hand[6] **c)** Barkan and Sheinin[7] **d)** Avlonitis[8] **e)** Tohidi[9] **f)** Sloan[11] **g)** Sloan and Koh[16] **h)** Hydrafact Software.

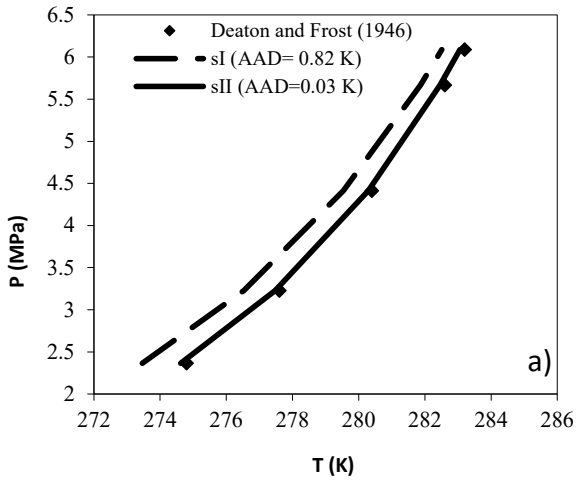
Deaton and Frost (1946)
sI (AAD= 0.82 K)
sII (AAD=0.03 K)
a)
P (MPa)
T (K)

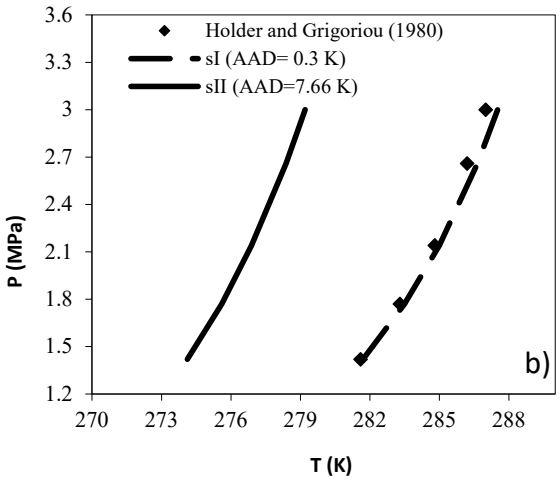
Holder and Grigoriou (1980)
sI (AAD= 0.3 K)
sII (AAD=7.66 K)
b)
P (MPa)
T (K)

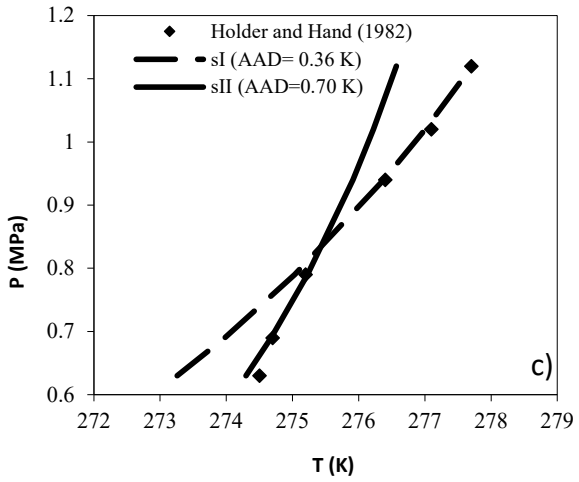
Holder and Hand (1982)
sI (AAD= 0.36 K)
sII (AAD=0.70 K)
c)
P (MPa)
T (K)

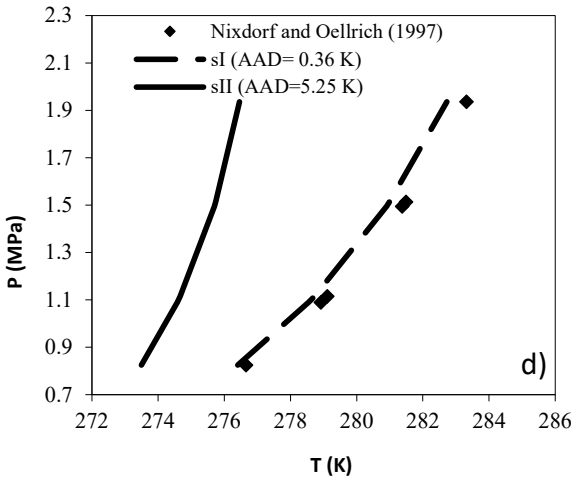
Nixdorf and Oellrich (1997)
sI (AAD= 0.36 K)
sII (AAD=5.25 K)
d)
P (MPa)
T (K)

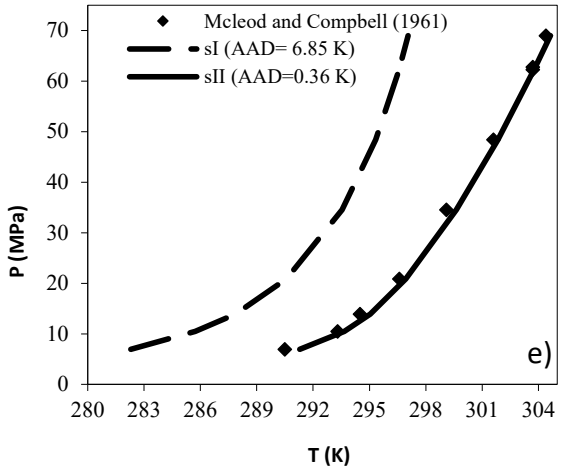
Mcleod and Compbell (1961)
sI (AAD= 6.85 K)
sII (AAD=0.36 K)
e)
P (MPa)
T (K)

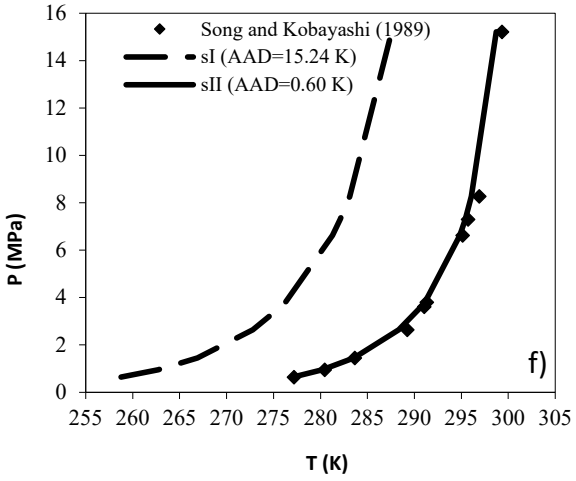
Song and Kobayashi (1989)
sI (AAD=15.24 K)
sII (AAD=0.60 K)
f)
P (MPa)
T (K)

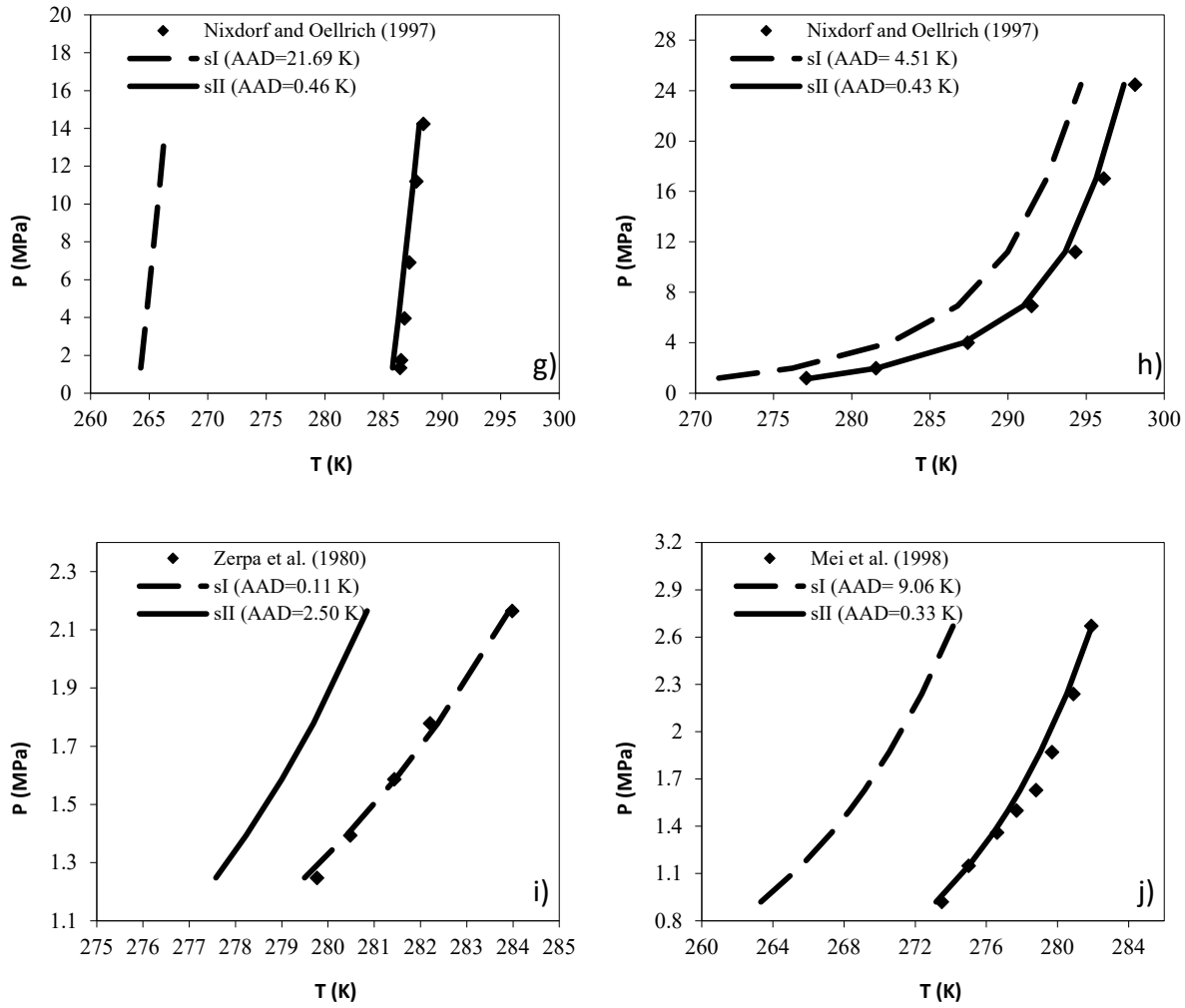

Figure 4. Hydrate dissociation conditions of different gas mixtures predicted using Kihara potential function parameters optimized in this work: **a)** 97.8 mole % C_1 + 2.2 mole % C_2, **b)** 17.7 mole % C_1 + 82.3 mole % C_2, **c)** 74 mole % C_2 + 26 mole % C_3, **d)** 85.15 mole % C_2 + 14.85 mole % C_3, **e)** 96.5 mole % C_1 + 3.5 mole % C_3, **f)** 88.13 mole % C_1 + 11.87 mole % C_3, **g)** 8.7 mole % C_1 + 91.3 mole % iC_4, **h)** 84.52 mole % C_1 + 12.55 mole % C_2 + 2.93 mole % C_3, **i)** 70.5 mole % C_2 + 17.4 mole % C_1 + 12.1 mole % C_3, **j)** 97.25 mole % C_1 + 1.42 mole % C_2 + 1.08 mole % C_3 + 0.25 mole % iC_4.